Copyright © 2014 Tech Science Press CMES, vol.99, no.3, pp.209-231, 2014

Stochastic Finite Element Method Reliability Analysis of the Corrugated I-beam Girder

Damian Sokolowski[1], **Marcin Kamiński**[2] **and Michal Strąkowski**[1]

Abstract: The main issue in this paper is to present stochastic analysis of the steel plate girder with the corrugated web subjected to Gaussian random fluctuations in its web thickness. Such an analysis is carried out using the Stochastic Finite Element Method based on the generalized stochastic perturbation technique and discretization of structure with the quadrilateral 4-noded shell finite elements. It is numerically implemented using the FEM system ABAQUS and the symbolic algebra system MAPLE, where all the probabilistic procedures are programmed. We compare the perturbation-based results with these obtained from traditional Monte-Carlo simulation and, separately, analytical solution calculated by a symbolic integration carried out in MAPLE. We calculate probabilistic characteristics of up to the fourth order for the static deformations and stresses, critical loads and eigenfrequencies to verify their distributions affected by the Gaussian dispersion of the web thickness itself resulting from an extensive corrosion, for instance. The reliability index for deformations is calculated according to the First Order Reliability Method (FORM) and can be further used in durability prediction of such structures.

Keywords: steel corrugated I-beam, Stochastic Finite Element Method, reliability analysis, stochastic perturbation technique, reliability index.

1 Introduction

A role of the corrugated I-beam girders still increases in the civil engineering practice [Johnson and Cafolla (1997); Sayed-Ahmed (2001)], while theoretical foundations as well as many numerical issues remain still mostly unresolved. They are

[1] Faculty of Civil Engineering, Architecture and Environmental Engineering, Technical University of Lódź, Al. Politechniki 6, 90-924 Lódź, Poland.

[2] Head of Chair of Structural Reliability, Faculty of Civil Engineering, Architecture and Environmental Engineering, Technical University of Lódź, Al. Politechniki 6, 90-924 Lódź, Poland.
Email: Marcin.Kaminski@p.lodz.pl
Webpage: http://www.kmk.p.lodz.pl/pracownicy/kaminski/index.htm

right now most frequently used as the homogeneous steel large span bridge girders as well as composite bridge girders, where the flanges are made of a concrete [He, Liu, Chen and Yoda (2012a, 2012b); Huang, Hikosaka and Komine (2004)]. As it is verified in this study, some theoretical models valid for Euler-Bernoulli beams approximate elastic behavior of the corrugated beams rather well, but sometimes, especially for the shear stresses analysis, they may be quite inefficient. Modern studies in this particular area obey the I-beams with both continuous and perforated webs [Ellobody (2011); Kiymaz, Coskun, Cosgun, and Seckin (2010)] that are done in theoretical, experimental as well as especially frequently, numerical way. Computational analysis, even in the deterministic context, is complex as the longitudinal waviness and vertical slenderness of the web together with the length of the structural element needs the very extended FEM discretization with preferably various order shell elements. So that an application of the Monte-Carlo simulation in probabilistic case looks extremely large time consuming one, also for a verification of its capacity in the elasto-static static regime. Stochastic Finite Element Method (SFEM) analysis of the structural elements is needed taking into account the statements of the engineering codes introducing a necessity of reliability index calculation – it is known that the corrugated I-beams are classified to the highest (risk) class of the reliability. It should be mentioned that the usage of SFEM approach to the steel structures is a relatively new idea [Graham and Siragy (2001); Waarts and Vrouwenvelder (1999)], not so extensively explored, and seems critically important, especially for determination of probabilistic characteristics of the critical force, pressure or a moment [Elishakoff (1983); Elishakoff (2000); Kamiński and Świta (2011); Luo and Edlund (1994)], decisive for their global stability loss or local deplanation. A choice of the input random variable of the local character, i.e. web thickness is driven by the experimental results concerning stochastic corrosion process of the I-beam girders [Papadopoulos, Stefanou and Papadrakakis (2009); Sadovský and Drdácký (2001)]. A verification whether output state functions have Gaussian distribution (or almost Gaussian) or not is important in the view of reliability index definition proposed in various norms as valid for the Gaussian variables by only. This formula follows directly the main philosophy of the First Order Reliability Method (FORM) [Cornell (1969); Melchers and Horwood (1987)] and cannot be simply extended towards other probability distributions, especially these that are non-symmetric [Murzewski (1989)]. Quite separate discussion concerns the modern available probabilistic techniques, where we usually consider simulation, fuzzy [Moller and Beer (2004)], spectral [Spanos and Ghanem (1991)] as well as the perturbation-based implementations [Kamiński (2013)] of the SFEM.

The main goal of this work is a presentation of the efficient numerical tool to validate stochastic time-independent reliability of the corrugated steel homogeneous

I-beam with uncertainty in its web thickness, which is most frequently driven by the corrosion scheme. It is done via the SFEM experiments, where the FEM itself is employed in some unusual way, because similarly to the polynomial chaos methods, it allows to recover some analytical function of the given output state parameters like maximum displacements, extreme stresses or the eigenvalues versus the input design variable, i.e. thickness of the girder. Such an idea implemented with the computer algebra system enables for an application of the variety of probabilistic techniques available in engineering practice. It is done through several FEM experiments with varying thickness value about its expected value (uniformly distributed around this expectation). The Weighted Least Squares Method (WLSM) enables to propose a polynomial form called the response function [Kamiński (2013)], to determine numerically its coefficients with the use of the Dirac-type distribution of the weights. A more detailed comparison in-between the weight types is available in [Kamiński (2011a)]. This approximation is further employed in three independent and parallel probabilistic procedures – analytical calculations of probabilistic moments and coefficients of the state functions, the Monte-Carlo simulation of these coefficients as well as stochastic perturbation technique determination of the uncertain structural behavior. It allows for a comparison of efficiency of these three various stochastic techniques applied to show finally the reliability index as a function of the input uncertainty level. Although the technique proposed and this specific example are both time-independent, it would be relatively easy to replace it with the time-dependent case study by engaging some time series representation of the corrosion process itself. Computational experiments are based on the FEM system ABAQUS employed together with the symbolic computing software MAPLE [Cornil and Testud (2004)] that shows quite efficient interoperability of symbolic and FEM programs.

2 Mathematical foundations

Let us analyze the expected values of any state function $f(b)$ by its expansion via Taylor series as follows [Kamiński (2007); Kamiński (2011b); Kamiński and Szafran (2010); Kleiber (1986)]:

$$E\left[f\left(b\right)\right]=\int_{-\infty}^{+\infty}f\left(b\right)p_{b}\left(x\right)dx=\int_{-\infty}^{+\infty}\left\{f^{0}\left(b\right)+\sum_{n=1}^{\infty}\frac{1}{n!}\varepsilon^{n}\frac{\partial^{n}f}{\partial b^{n}}\left(\Delta b\right)^{n}\right\}p_{b}\left(x\right)dx \tag{1}$$

Of course, an expansion is carried out over the finite number of components to assure satisfactory accuracy. Analytical derivation of the expected values for the structural response according to the general 10^{th} order expansion proceeds for the

Gaussian variables using the following formula:

$$E\left[f\left(b\right)\right]=f^{0}\left(b\right)|_{b=b^{0}}+\frac{1}{2}\varepsilon^{2}\mu_{2}\left(b\right)\frac{\partial^{2}f}{\partial b^{2}}|_{b=b^{0}}+...+\frac{1}{10!}\varepsilon^{10}\mu_{10}\left(b\right)\frac{\partial^{10}f}{\partial b^{10}}|_{b=b^{0}} \tag{2}$$

Let us mention that we multiply here by the relevant order probabilistic moments of the input random variables to get the algebraic formulas in symbolic computations; the remaining second, third and fourth central probabilistic moments equations may be found in [Kamiński (2013)]. Therefore, this method in its generalized form is convenient for all the random distributions, where the above mentioned moments may be analytically derived (or at least computed for a specific combination of the parameters). Finally, one may recover the kurtosis and the skewness from their well-known definitions as

$$\kappa\left(f\left(b\right)\right)=\frac{\mu_{4}\left(f\left(b\right)\right)}{\sigma^{4}\left(f\left(b\right)\right)}-3,\qquad\beta\left(f\left(b\right)\right)=\frac{\mu_{3}\left(f\left(b\right)\right)}{\sigma^{3}\left(f\left(b\right)\right)}. \tag{3}$$

The reliability index for the particular state functions as

$$R\left(f\left(b\right)\right)=\frac{E\left[\hat{f}-f\right]}{\sigma\left(\hat{f}-f\right)} \tag{4}$$

where the pair $\left(\hat{f};f\right)$ denotes the admissible value of the given state function and its computed maximum counterpart (admissible and maximum vertical displacements). Some civil engineering codes state, for instance, that this difference cannot be smaller than 25% of the structural eigenfrequency, so that eqn (11) may serve for the straightforward estimation of the reliability for the structures subjected to the dynamic excitations.

3 Computational implementation by the RFM-FEM

3.1 Elastodynamics in the FEM notation

Let us consider the following equilibrium system [Clough and Penzien (1975); Kleiber (1986)]

$$\mathbf{M}^{\alpha}\mathbf{q}^{\alpha}+\mathbf{K}^{\alpha}\mathbf{q}^{\alpha}=\mathbf{Q}^{\alpha} \tag{5}$$

which represents equations of motion of the discretized system. We complete this equation usually with the component $\mathbf{C}^{\alpha}\mathbf{q}^{\alpha}$ so that

$$\mathbf{M}^{\alpha}\mathbf{q}^{\alpha}+\mathbf{C}^{\alpha}\mathbf{q}^{\alpha}+\mathbf{K}^{\alpha}\mathbf{q}^{\alpha}=\mathbf{Q}^{\alpha} \tag{6}$$

and we decompose the damping matrix as

$$\mathbf{C}^{\alpha}=\alpha_{0}\mathbf{M}^{\alpha}+\alpha_{1}\mathbf{K}^{\alpha}, \tag{7}$$

where the coefficients α_0 and α_1 are determined using the specific eigenfunctions for this problem. Then, the following equation is solved numerically:

$$\mathbf{M}^{\alpha}\mathbf{q}^{\alpha} + \alpha_0\mathbf{M}^{\alpha}\mathbf{q}^{\alpha} + \alpha_1\mathbf{K}^{\alpha}\mathbf{q}^{\alpha} + \mathbf{K}^{\alpha}\mathbf{q}^{\alpha} = \mathbf{Q}^{\alpha}, \tag{8}$$

where no summation over the doubled indices α is applied here. Of course, the undamped free vibrations are described by the following algebraic system:

$$\mathbf{M}^{\alpha}\mathbf{q}^{\alpha} + \mathbf{K}^{\alpha}\mathbf{q}^{\alpha} = \mathbf{0} \tag{9}$$

and the harmonic solution $\mathbf{q}^{\alpha} = \mathbf{A}^{\alpha}\sin\omega_{\alpha}t$ leads to the relation

$$-\mathbf{M}^{\alpha}\mathbf{A}^{\alpha}\omega_{\alpha}^2\sin\omega_{\alpha}t + \mathbf{K}^{\alpha}\mathbf{A}^{\alpha}\sin\omega_{\alpha}t = \mathbf{0}. \tag{10}$$

There holds for $\sin\omega_{\alpha}t \neq \mathbf{0}$ and for $\mathbf{A}^{\alpha} \neq \mathbf{0}$

$$-\mathbf{M}^{\alpha}\omega_{\alpha}^2 + \mathbf{K}^{\alpha} = \mathbf{0}. \tag{11}$$

Let us note that some previous solutions to the eigenvalue problems with random parameters are available in [Collins and Thomson (1969); Mironowicz and Śniady (1987); Shinozuka and Astill (1972)], but out of the stochastic perturbation technique, whose second order second moment approach to this matter is available since many years. Obviously, eqn (26) for the time independent generalized coordinates returns the well-known linear statics equilibrium systems for the RFM as follows [Kamiński (2007); Kamiński and Szafran (2010)]

$$\mathbf{K}^{\alpha}\mathbf{q}^{\alpha} = \mathbf{Q}^{\alpha}. \tag{12}$$

3.2 Elastic stability matrix equations

The deformation energy of the finite element idealizing elastic behavior is introduced for the 3D Cartesian system as

$$U^{(\alpha)} = \frac{1}{2}\mathbf{q}_{(\alpha)}^{T}\mathbf{k}_{(\alpha)}^{(s)}\mathbf{q}_{(\alpha)} + \frac{1}{2}\mathbf{q}_{(\alpha)}^{T}\mathbf{k}_{(\alpha)}^{(\sigma)}\mathbf{q}_{(\alpha)} \tag{13}$$

where $\mathbf{q}_{(\alpha)}$ is the nodal displacements vector, $\mathbf{k}_{(\alpha)}^{(s)}$ is the elemental elastic stiffness matrix and $\mathbf{k}_{(\alpha)}^{(\sigma)}$ stands for the geometric stiffness matrix of this element. So that, potential energy for this finite element may be expressed as

$$J_P^{(\alpha)} = \frac{1}{2}\mathbf{q}_{(\alpha)}^{T}\left(\mathbf{k}_{(\alpha)}^{(s)} + \mathbf{k}_{(\alpha)}^{(\sigma)}\right)\mathbf{q}_{(\alpha)} - \mathbf{R}_{(\alpha)}^{T}\mathbf{q}_{(\alpha)} \tag{14}$$

whose minimization with respect to the generalized displacement vector leads to

$$\left(\mathbf{k}_{(\alpha)}^{(s)}+\mathbf{k}_{(\alpha)}^{(\sigma)}\right)\ \mathbf{q}_{(\alpha)}=\mathbf{R}_{(\alpha)}. \tag{15}$$

The global stability equation is usually formulated as

$$\left(\mathbf{K}_{(\alpha)}^{(s)}+\lambda_{(\alpha)}\mathbf{K}_{(\alpha)}^{(\sigma)}\left(\hat{F}_{(\alpha)}\right)\right)\ \mathbf{r}_{(\alpha)}=\lambda_{(\alpha)}\hat{\mathbf{R}}_{(\alpha)}, \tag{16}$$

where $\mathbf{K}_{(\alpha)}^{(\sigma)}\left(\hat{F}_{(\alpha)}\right)$ is the series of geometric stiffness matrices, $\mathbf{K}_{(\alpha)}^{(s)}$ stands for the series of the elastic stiffness matrices, the loading series $\mathbf{R}_{(\alpha)}$ have proportional character to $\lambda_{(\alpha)}\hat{\mathbf{R}}_{(\alpha)}$, where $\lambda_{(\alpha)}$ is the loading factor series and $\hat{\mathbf{R}}_{(\alpha)}$ is some external loading. Further, the distribution of internal forces $\hat{\mathbf{F}}_{(\alpha)}$ is equivalent to the load $\hat{\mathbf{R}}_{(\alpha)}$ and displacement $\mathbf{r}_{(\alpha)}$ is equivalent to the load $\lambda_{(\alpha)}\hat{\mathbf{R}}_{(\alpha)}$. We determine the values of $\lambda_{(\alpha)}$ from the following condition:

$$\left\{\begin{array}{l}\left(\mathbf{K}_{(\alpha)}^{(s)}+\lambda_{(\alpha)}\mathbf{K}_{(\alpha)}^{(\sigma)}\left(\hat{F}_{(\alpha)}\right)\right)\ \mathbf{r}_{1(\alpha)}=\lambda_{(\alpha)}\hat{\mathbf{R}}_{(\alpha)}\\ \left(\mathbf{K}_{(\alpha)}^{(s)}+\lambda_{(\alpha)}\mathbf{K}_{(\alpha)}^{(\sigma)}\left(\hat{F}_{(\alpha)}\right)\right)\ \mathbf{r}_{2(\alpha)}=\lambda_{(\alpha)}\hat{\mathbf{R}}_{(\alpha)}\end{array}\right.\ ,\mathbf{r}_{1(\alpha)}\neq\mathbf{r}_{2(\alpha)},\mathbf{r}_{1(\alpha)}-\mathbf{r}_{2(\alpha)}=\mathbf{v}_{(\alpha)}, \tag{17}$$

so that we obtain the basic algebraic equation series representing elastic stability as the certain eigenvalue problem

$$\left(\mathbf{K}_{(\alpha)}^{(s)}+\lambda_{(\alpha)}\mathbf{K}_{(\alpha)}^{(\sigma)}\left(\hat{F}_{(\alpha)}\right)\right)\ \mathbf{v}_{(\alpha)}=0. \tag{18}$$

Therefore, the basic condition that one can get for the critical value $\lambda_{(\alpha)}=\lambda_{cr(\alpha)}$ and for critical load $\mathbf{R}_{cr(\alpha)}=\lambda_{cr(\alpha)}\hat{\mathbf{R}}_{(\alpha)}$ is the following one:

$$\det\left(\mathbf{K}_{(\alpha)}^{(s)}+\lambda_{(\alpha)}\mathbf{K}_{(\alpha)}^{(\sigma)}\left(\hat{F}_{(\alpha)}\right)\right)=0. \tag{19}$$

4 Computational analysis

Simply supported steel corrugated web I beam girder with a span of 40.0 m is examined with the use of FEM system ABAQUS (Figs. 1-3). We apply the dead load of the girder and normative load coming from the vehicles $15.0kN/m^2$ collected from a half of the 20.0 m bridge width ($184.16kN/m$). A torsion induced by the eccentricity of the uniform load from a mass center of the girder is neglected in the model. The structural steel used to form the plate girder is S460 M/ML with Poisson ratio ν=0.3, shear modulus G=80 GPa and Young modulus equal to 210 GPa. The FEM simulations are based upon the full-scale 3D model of the girder

developed with its quadrilateral 4-noded 100.800 linear thin shell finite elements as well as 221.200 uniformly distributed nodal points. We postpone the local thickness changes resulting from the welds in-between the web and flanges; the detailed discretization into the four-noded shell finite elements is presented in Fig. 4.

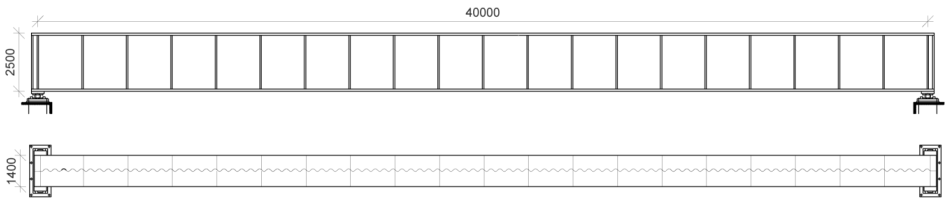

Figure 1: Layout of the girder.

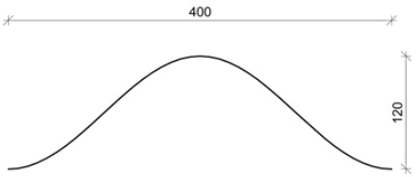

(25)

$$f(x) = 6\sin\left(\frac{\pi x}{20}\right) \quad [cm]$$

Figure 2: Corrugated web pattern [mm]

The Gaussian input random parameter is web thickness (according to the possible corrosion process) with the expectation equal to $E[t_w] = 56\ mm$ and coefficient of variation fluctuating within the interval $\alpha(t_w) \in [0.00, 0.25]$. A spectrum of the web thicknesses necessary to build the response functions according to the WLSM algorithm ranges from 51 to 61 mm with 1 mm difference between each FEM model. We analyze sequentially extreme values the following state parameters necessary in structural reliability of this girder: deflection (f), normal stress (σ_{max}), reduced Huber-Mises stress (σ_{red}) in global maximum, as well as the eigenfrequencies and critical loads of the girder. Some comparison of the deterministic results computed via analytical and FEM models are collected in Table 1.

Computer analysis for determination of the eigenfrequencies is performed with the use of an active non-linear geometry option in the system ABAQUS, where Lanc-

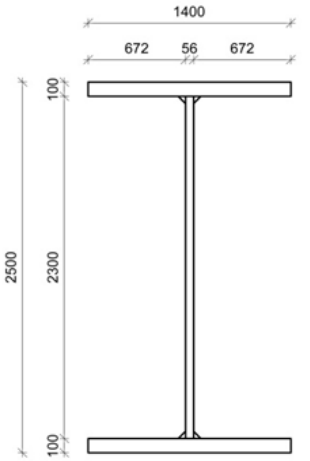

Figure 3: Dimensions of the cross-section [mm].

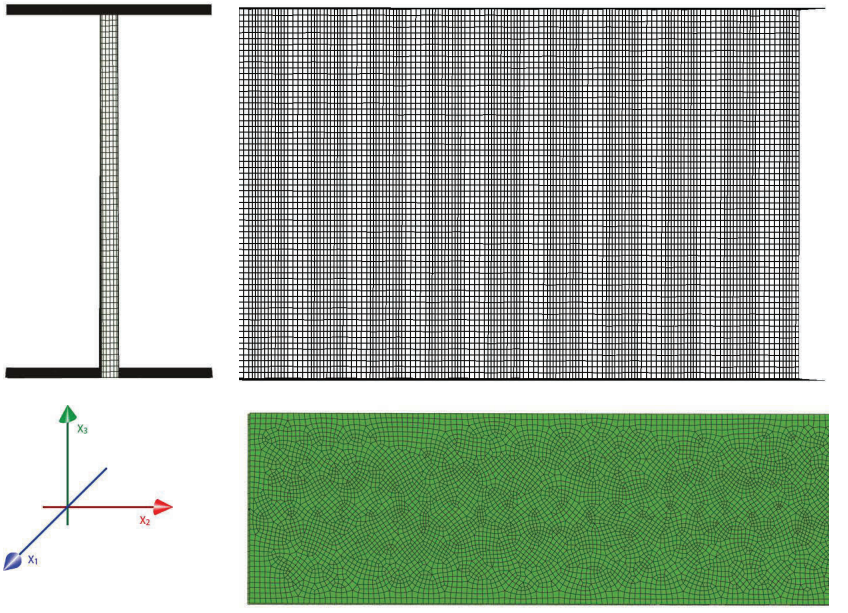

Figure 4: ABAQUS discretization of the girder.

zos algorithm is applied with restriction to the first 10 eigenfrequencies and with symmetric matrix storage; friction-induced damping effects are not postponed. All the first ten eigenfrequencies and critical load values computed in ABAQUS are listed in Table 2. Stability analysis needs the asymmetric matrix storage, where the subspace eigensolver for a determination of the first four buckling modes is chosen. The critical load (CL) is evaluated as

$$CL = \frac{q_{crit} - q_{initial}}{q_{initial}} = \frac{q_{\max}}{q_{initial}} - 1 \tag{20}$$

Table 1: Comparison of the results from FEM simulations and analytical calculus.

tw	Critical load		Eigenfrequency [Hz]		f [cm]	
	Analytical	Computation	1st Analytical	4th Computation	Analytical	Computation
51	4,805	4,3979	5,008	4,9282	7,12	7,126
52	4,805	4,4087	4,992	4,9172	7,12	7,117
53	4,805	4,4195	4,976	4,9061	7,11	7,108
54	4,805	4,4305	4,961	4,8951	7,13	7,1
55	4,806	4,4415	4,946	4,8841	7,14	7,091
56	**4,806**	**4,4526**	**4,931**	**4,8731**	**7,14**	**7,084**
57	4,806	4,4638	4,916	4,8623	7,15	7,076
58	4,806	4,4751	4,901	4,8515	7,16	7,069
59	4,806	4,4866	4,887	4,8407	7,16	7,061
60	4,806	4,4982	4,872	4,8301	7,17	7,054
61	4,806	4,5099	4,858	4,8195	7,17	7,048

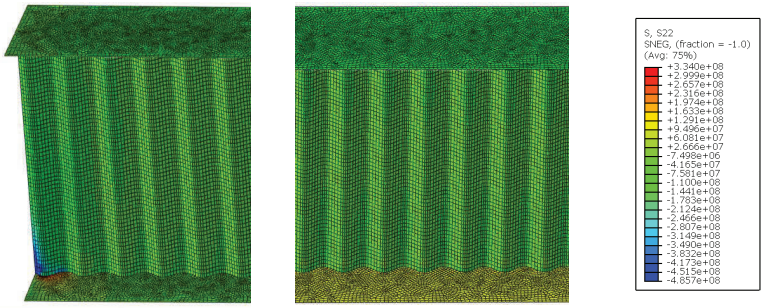

Figure 5: Normal stresses (σ_{22}) distribution at the support (left) and in the middle of the span (right).

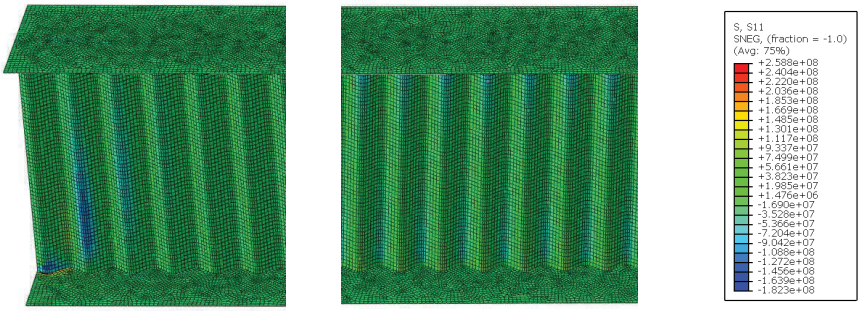

Figure 6: Normal stresses (σ_{11}) distribution at the support (left) and in the middle of the span (right).

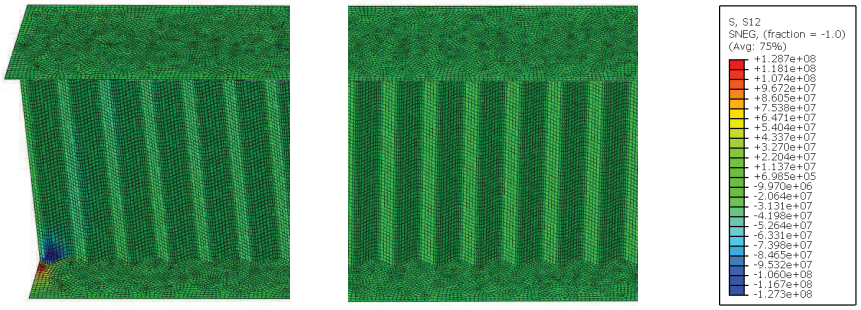

Figure 7: Shear stresses (σ_{12}) distribution at the support (left) and in the middle of the span (right).

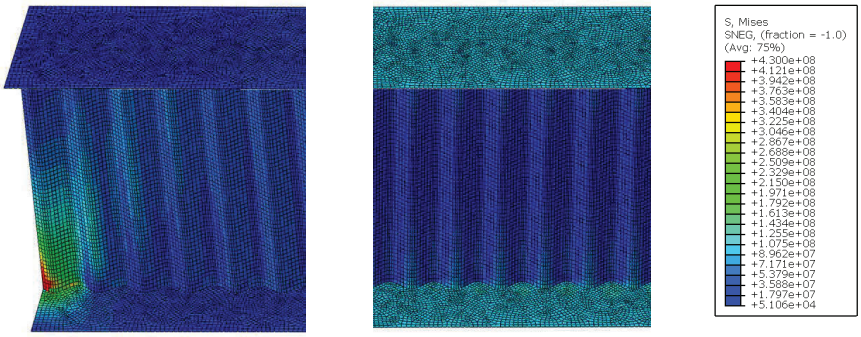

Figure 8: Reduced stresses from von Mises hypothesis at the support (left) and in the middle of the span (right).

Table 2: FEM-based eigenfrequencies and critical loads vs. web thickness.

t_w	Critical loads				Eigenfrequencies [Hz]									
	1st form	2nd form	3rd form	4th form	1st mode	2nd mode	3rd mode	4th mode	5th mode	6th mode	7th mode	8th mode	9th mode	10th mode
51	4,3979	5,7446	9,1377	13,019	1,3948	3,0305	3,3097	4,9284	5,6914	9,2259	11,74	17,035	18,196	21,622
52	4,4087	5,8038	9,2688	13,109	1,3949	3,035	3,3111	4,9172	5,6986	9,2056	11,728	17,018	18,149	21,588
53	4,4195	5,8624	9,3981	13,197	1,395	3,0392	3,3129	4,9061	5,7058	9,1856	11,716	17	18,103	21,554
54	4,4305	5,9206	9,5255	13,283	1,3951	3,0429	3,3154	4,8951	5,713	9,1656	11,704	16,975	18,063	21,128
55	4,4415	5,9784	9,6511	13,366	1,3951	3,0463	3,3173	4,8841	5,7203	9,1462	11,693	16,962	18,012	21,488
56	**4,4526**	**6,0357**	**9,7751**	**13,448**	**1,395**	**3,0493**	**3,32**	**4,8731**	**5,7276**	**9,1268**	**11,682**	**16,943**	**17,967**	**21,456**
57	4,4638	6,0926	9,8975	13,529	1,395	3,052	3,323	4,8623	5,7349	9,1077	11,671	16,923	17,923	21,424
58	4,4751	6,1492	10,0185	13,609	1,3949	3,0545	3,3263	4,8515	5,7423	9,0888	11,66	16,903	17,879	21,393
59	4,4866	6,2054	10,1379	13,688	1,3949	3,0566	3,3299	4,8407	5,7497	9,0702	11,65	16,882	17,835	21,362
60	4,4982	6,2613	10,2561	13,767	1,3947	3,0585	3,3337	4,8301	5,7572	9,0518	11,64	16,681	17,792	21,332
61	4,5099	6,3168	10,3729	13,846	1,3946	3,0301	3,3377	4,8195	5,7647	9,0336	11,631	16,84	17,75	21,302

A comparison of the FEM results and these based on the fundamentals of the strength of materials relevant to the I-beams with the constant cross-section shows first that the deflections resulting from analytical calculations are apparently larger than these obtained in the FEM analysis with the waviness (with about 10%). It is very interesting that maximum deflection increases in an analytical model with the straight web – the web increases a little bit faster than its stiffness; computational model with the sinusoidal web shows an opposite tendency. It needs to be underlined that all the differences and fluctuations are smaller than a percent or two, so generally may be neglected. The critical load magnitude shows analogous interrelations as analytical method results in an overestimation of the stability loss and almost lack of sensitivity to the web thickness. Stability limit obtained with the ABAQUS increases moderately and systematically together with the web thickness. Eigenfrequency analysis gives slightly different result as both series decrease together with an increase of the web thickness, where analytical technique overestimates the final value; nevertheless, both methods return very similar values here. Further results are presented in Figs. 5-8 and they are focused on normal stresses distributions σ_{22}, σ_{11}, shear stresses σ_{12} as well as on the reduced von Mises stresses. They show a dominant role of the longitudinal normal stresses giving the largest contribution to the reduced stresses. Shear stresses fluctuations are noticed in a bottom of the first waves of the girder (at the left and at the right hand sides) – so that they need to be stiffened additionally to optimize the entire structure. All these stresses are in the same range of a magnitude and have distributions similar to these calculated for the girder with the straight web (except the existence of the normal stresses σ_{11} in this model).

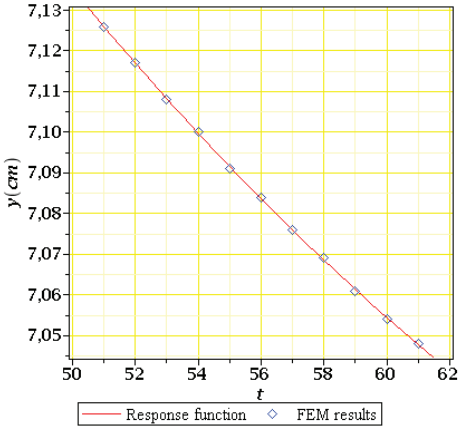

Figure 9: Maximum deflection vs. web thickness.

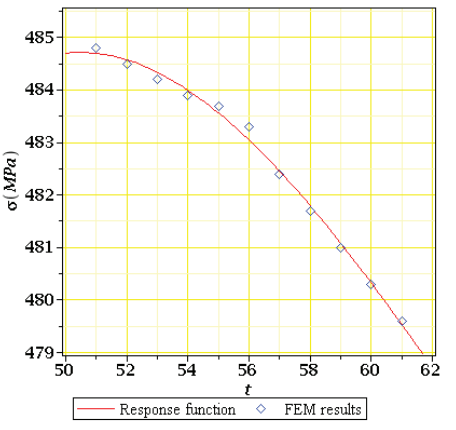

Figure 10: Maximum stresses vs. web thickness.

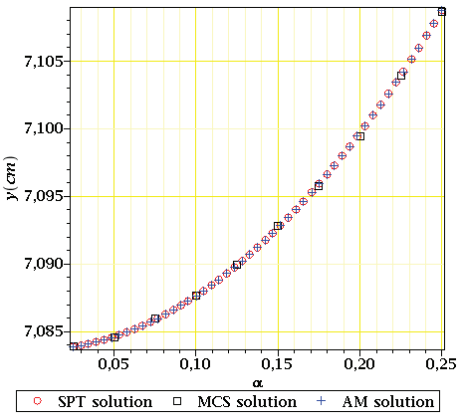

Figure 11: Expectations of the maximum deflection.

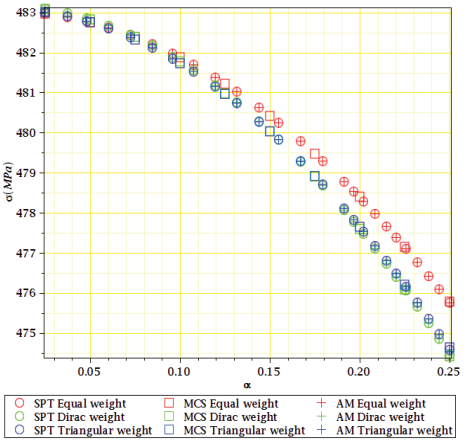

Figure 12: Expectations of the maximum stresses for different types of weights.

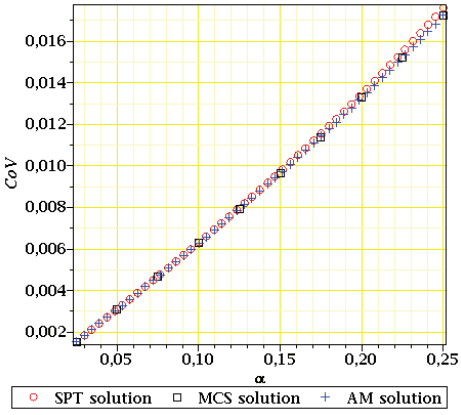

Figure 13: CoV of the maximum deflection.

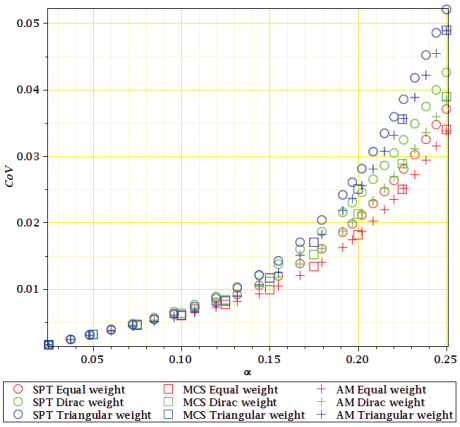

Figure 14: CoV of the maximum stresses for different types of weights.

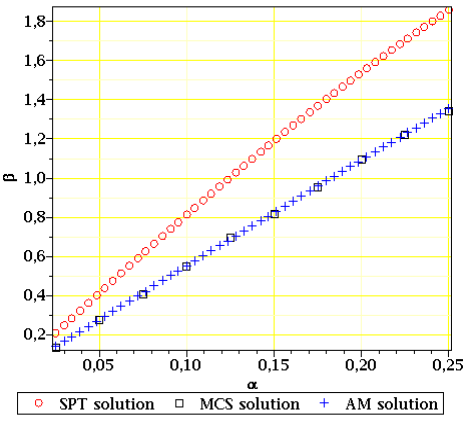

Figure 15: Skewness of the maximum deflection.

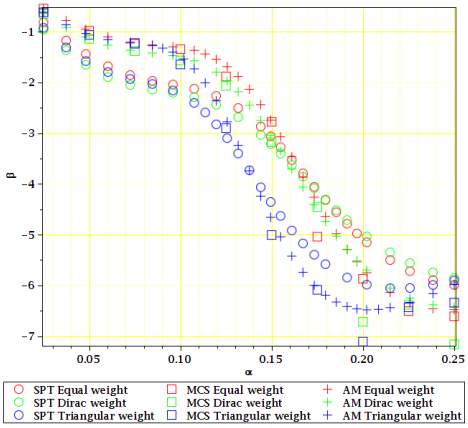

Figure 16: Skewness of the maximum stresses for different types of weights.

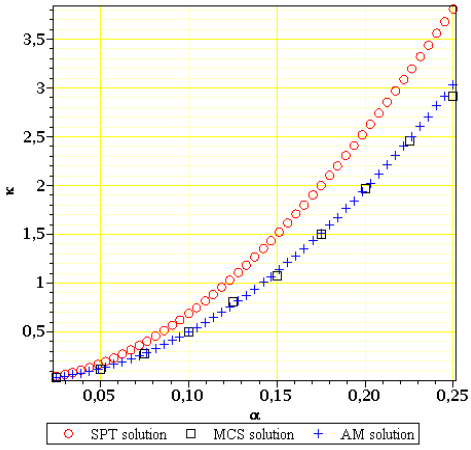

Figure 17: Kurtosis of the maximum deflection.

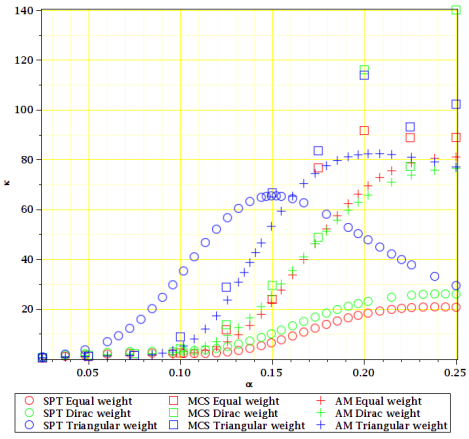

Figure 18: Kurtosis of the maximum reduced stresses for different types of weights.

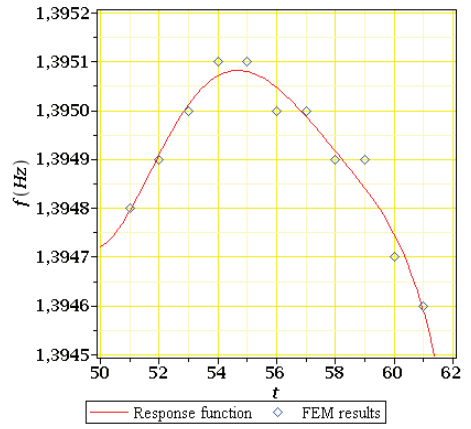

Figure 19: First eigenfrequency mode vs. web thickness.

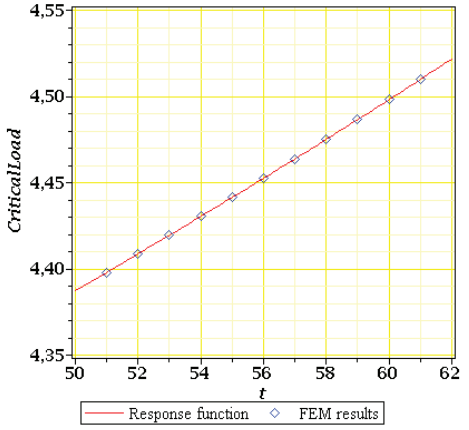

Figure 20: Critical load relative to initial load vs. web thickness.

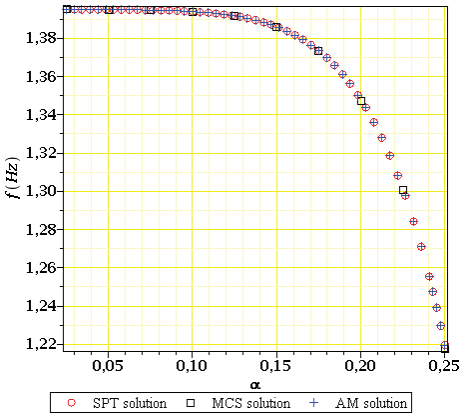

Figure 21: Expectations of the first eigenfrequency.

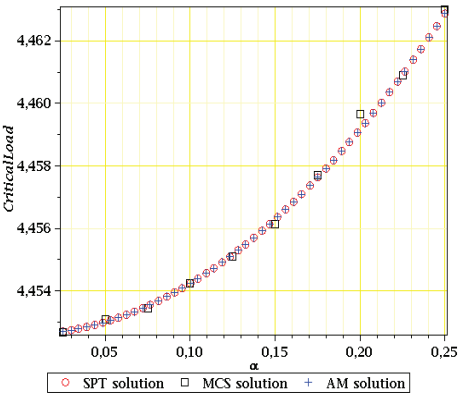

Figure 22: Expectations of the critical load.

Further MAPLE results provided in Figs. 19-28 show in turn two response functions, i.e. first eigenfrequency and the first critical load versus web thickness (Figs. 19-20) as well as, in pairs, expectations (Figs. 21-22), coefficients of variation (Figs. 23-24), skewnesses (Figs. 25-26) and kurtosis (Figs. 27-28). All the probabilistic quantities are plotted as the functions of the input coefficient of variation. The first eigenfrequency is almost insensitive to the web thickness and these irregular fluctuations result in a strong oscillations of higher order statistics here. The basic critical load is linearly dependent upon this thickness and result in a very regular and predictable probabilistic moments. Expectations of both of them are exactly the same in all the three methods, but while the eigenfrequency decreases, the critical load increases (both in a nonlinear manner). The output coefficient of variation for the critical load depends linearly upon the input one and all numerical methods agree with each other (the range is the same as before in Figs. 13-14). It means that (cf. Figs. 20 and 24) the resulting critical load may be treated as the Gaussian variable. The same coefficient observed for the eigenfrequency increases dramatically and exponentially for larger values of $\alpha(t_w)$ and gives smaller values in the perturbation-based computations; it is strongly affected by the response function and all the trial points. Higher order statistics underline these facts in a very apparent way – these corresponding to the eigenfrequency (Figs. 25 and 27) are irregular, diverge and show extreme values exceeding usual interval, especially for larger input CoVs, while these adjacent to the lowest stability limit are almost linear and keep rather close to 0. Finally, different numerical methods are significantly distant from each other in eigenfrequency analysis, while stability verification gives close results in analytical, perturbation-based and simulation probabilistic analyses.

A final part of numerical experiments is strictly devoted to probabilistic analysis and is carried out using three independent techniques, i.e. Monte-Carlo simulation (MCS), stochastic perturbation technique (SPT) as well as the semi-analytical method (AM). Each of these methods is based on initial determination of the response function of the given state parameter with respect to the uncertain thickness using the above tables. Monte-Carlo analysis proceeds here with 500.000 random trials performed for α=0.025,0.050,...,0.25 using polynomial response functions, while the perturbation technique uses full 10^{th} order Taylor expansion for all up to the fourth order probabilistic characteristics; analytical calculus consists in a symbolic integration of the response polynomials embedded into the classical probability definitions. Therefore, the first method returns a discrete set of values, while the two remaining approaches – the continuous variability curves for $\alpha \in [0.00, 0.25]$; α=0 serves for a verification since all the methods need to return 0.0 here as for the deterministic test. We study each time the response functions, expectations, coefficients of variations, skewnesses as well as kurtosis of the maximum displacements and stresses decisive for the ULS and SLS limit conditions. The adjacent numerical results are shown in Figs. 9-18, where the response functions (Figs. 9-10) are given with respect to the mean web thickness, while probabilistic moments and coefficients (Figs. 11-18) – with respect to the input coefficient of variation. We provide additionally a comparison of three different types of the weights distribution in the WLSM scheme – (a) constant over the input variability interval, (b) triangular as well as (c) Dirac-type during the computations of probabilistic characteristics for the extreme reduced stresses (Figs. 12, 14, 16 and 18). Numerical values corresponding to these distributions are (a) [1,1,1,1,1,1,1,1,1,1,1], (b) [1,2,3,4,5,6,5,4,3,2,1] and, finally, (c) [1,1,1,1,1,6,1,1,1,1,1]. These different weights are inserted into all the probabilistic numerical methods to verify an interrelation in-between the WLSM and perturbation, simulation and the analytical symbolic integration procedures.

It is apparent from our computational evidence that both datasets coming from the FEM experiments are a little bit irregular, so that the polynomial response functions are somewhat distant from these points, however are continuous, smooth and with no local oscillations; generally, according to an engineering intuition, the values of both functions decrease together with an increasing value of the web thickness. The expectations are not so regular – especially these computed for the maximum deflection. It should be underlined that the results given in Figs. 9-10 do not remain in any contradiction with these included in Figs. 11-12 because the expectations as well as all the remaining probabilistic characteristics are determined with respect to the input coefficients of variation. The expectations of the displacements monotonously increase, while the expected values of stresses decrease in a simi-

lar way together with an increase of the input random deviation; all the numerical methods return here perfectly the same values independently of input randomness. The output coefficients of variation (Figs. 13-14) almost do not depend on the evaluation method and quite naturally increase proportionally to the input α. However, these corresponding to the displacements increase linearly, while the CoVs of stresses are apparently nonlinear. The very important fact is that the final values of this coefficient are significantly smaller for displacements and reduced stresses than for the corresponding input random thickness. It would remarkably affect the reliability index for extensively corroded structural elements, where input CoV may be out of the range adopted here. Higher order probabilistic coefficients like skewness (Figs. 15-16) and kurtosis (Figs. 17-18) loose a perfect agreement in-between all numerical methods – analytical solution is very close to the simulation-based one. The perturbation-based SFEM returns however skewness of a similar character to these two techniques, whereas kurtosis is significantly underestimated by the proposed SFEM solution. Taking into account these results one can conclude that the final limit functions responsible for both ULS and SLS are rather non-Gaussian and need more extended reliability index equation than this provided now in Eurocode 0. It remains clear that the 10^{th} order Taylor expansion is quite sufficient for determination of the first two probabilistic moments, while higher order calculations may need more effort and attention in the context of the perturbation method since the differences detected especially for larger input coefficients of variation. It is documented by the extended results contained in Figs. 12, 14, 16 and 18 that the distribution of the weights inside a computational domain adjacent to the WLSM scheme has very limited influence on the chosen and documented probabilistic characteristics. Some more apparent variations are noticed for kurtosis (Fig. 18), however they are all very distant from 0, so that do not affect qualitatively any conclusion made on its basis. Nevertheless, we prefer the Dirac type distribution scheme as it strongly highlights the structural output computed for the expectation of the Gaussian random input, which in some way reflects the basic idea behind the Taylor expansion, even in a traditional deterministic context.

This limitation of course does not affect in any way the reliability index calculated via these three numerical methods and shown in Fig. 24 also as a function of the input coefficient of variation of t_w. Since an initial design is rather optimal, then the values obtained here are very close to the lower limits specified by the Eurocode 0 (from about 3.0 up to 5.0). It is typical that this index decreases almost exponentially together with an increasing input CoV and of course that its value is independent of a computational technique employed. Although this numerical example is the time-independent one, one can replace input CoV with the time parameter according to some well-known aging rules and then, this reliability curve will remain

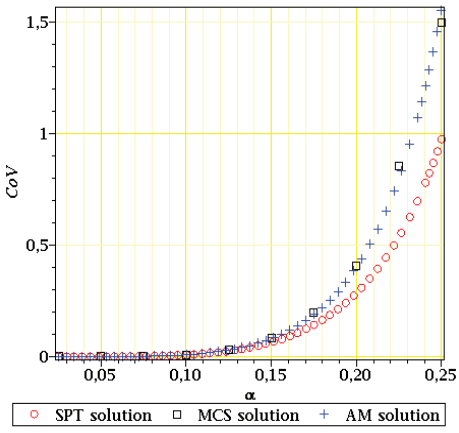

Figure 23: CoV of the first eigenfrequency.

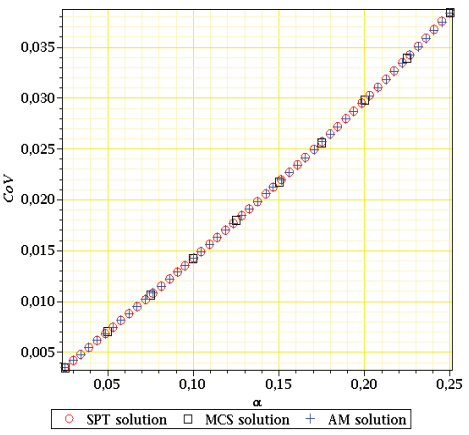

Figure 24: CoV of the critical load.

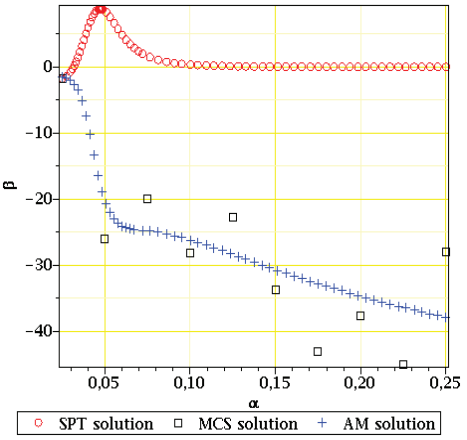

Figure 25: Skewness of the first eigenfrequency.

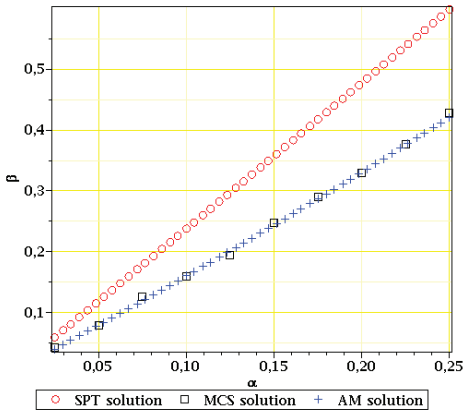

Figure 26: Skewness of the critical load.

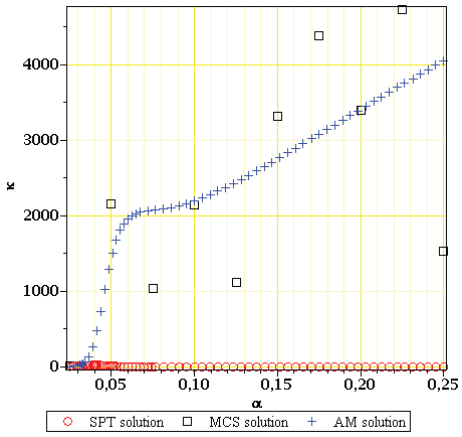

Figure 27: Kurtosis of the first eigenfrequency.

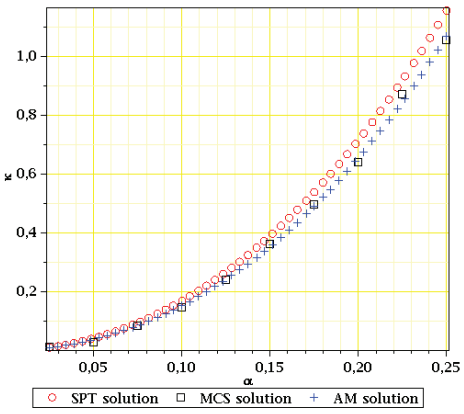

Figure 28: Kurtosis of the critical load.

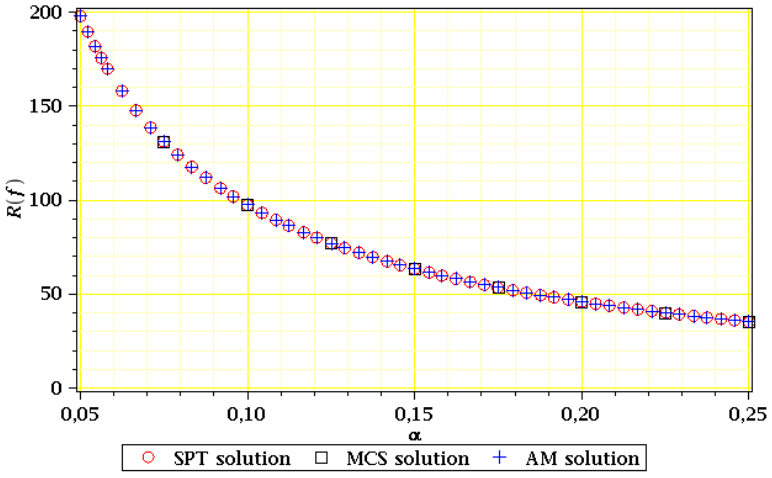

Figure 29: Reliability index of the corrugated I-beam.

almost the same. In a general conclusion, it is demonstrated here that the optimally designed corrugated I-beam is almost on its reliability limit given by Eurocode 0 when some remarkable uncertainty appears in its web thickness (as usually in steel bridge structures), even with a local character. Therefore, corrosion protection of rationally designed corrugated I-beams is of the paramount importance considering their stochastic reliability and durability. The very interesting effect is remarkable in Figs. 25 and 27 – the oscillatory character of the results coming from the Monte-

Carlo simulation in addition to the principal trends provided by the analytical solution; they can be recognized in smaller scale for the coefficients of variation given in Fig. 23 also. The major source of these discrepancies follows most probably Fig. 19, where we observed the very similar eigenfrequencies for the neighboring web thicknesses values. The second reason could be extremely large values of the skewness and kurtosis themselves counted here in hundreds, which is completely unusual for the remaining state functions. The fluctuations of higher order statistics computed for the reduced stresses according to both stochastic perturbation and analytical method remains also a little bit different than in the other cases as the convexity of these characteristics may not be preserved for the entire domain of the input coefficient of variation – usually these functions were convex or concave unlike in case of the first eigenfrequency, where we observe some sign fluctuations for the second derivative with respect to the input uncertainty source and different character for different numerical techniques (unusual also).

5 Concluding remarks

1. Summarizing, the article presents an extensive stochastic analysis of the corrugated-web girder simulated with use of the full-scale FEM 3D model based on the rectangular shell finite elements, including the reliability index β as well as up to the fourth order probabilistic moments and coefficients of the given state parameters. An initial deterministic comparison of the computational and analytical deterministic methods show good consistence of both methods in a modeling of maximum displacements, critical loads and eigenvalues.

2. The Stochastic perturbation-based Finite Element Method seems to be precise for the first two probabilistic moments and, at the same time, for reliability index adjacent to the Gaussian random variables, while conditionally efficient for skewness and kurtosis determination – for the input CoV smaller or equal to 0.10. This fact has been verified through stochastic parametric tests in a comparison to the analytical and simulation-based probabilistic models. However, Gaussian variability of the web thickness returns non-Gaussian state parameters relevant to both ULS and SLS verification, so that these higher order statistics may become relevant when engineering codes will contain the additional reliability index equations.

3. Further computational modeling attentions, in both deterministic and stochastic context needs a connection area in-between the web and the flanges, where usually the weld is added. It changes initial geometry of this structure with this typically surface character and needs additional usage of some 3D

solid elements like tetrahedra or hexahedra. Their influence on the overall static uncertain response of the corrugated I-beam girder, structural imperfections in the welds themselves as well as fatigue fracture of these welds need separate SFEM analyses in the future. The very interesting aspect is the post-critical behavior of the steel structures, especially in the stochastic context (particularly of the SFEM), which really deserved further attention and research efforts [Steinböck, Jia, Höfinger, Rubin and Mang (2008)].

Acknowledgement: Computational FEM analysis has been carried out on the ABAQUS installation operated on the cluster MARS (IBM BladeCenterH with 5365,76 GFlops) in the Academic Computer Center CYFRONET in Cracow, Poland.

References

Clough, R.; Penzien, J. (1975): Dynamics of structures, McGraw-Hill, New York.

Collins, J.D; Thomson, W.T. (1969): The eigenvalue problem for structural systems with statistical properties, *AIAA J*, vol. 7, pp. 642-648.

Cornell, C.A. (1969): A first-order reliability theory for structural design. Study 3. Structural reliability and codified design. University of Waterloo Press, Waterloo.

Cornil, J.M.; Testud P. (2004): An introduction to Maple V, Springer-Verlag, Berlin.

Elishakoff, I. (1983): Probabilistic methods in the theory of structures, Wiley & Sons, New York.

Elishakoff, I. (2000): Uncertain buckling: its past, present and future. *Int J Sol & Struct*, vol. 37, pp. 6869-6889.

Ellobody, E. (2011): Interaction of buckling modes in castellated steel beams. *J Constr Steel Res,* vol. 67, pp. 814–825.

Erfani, T.; Utyuzhnikov, S.V. (2012): Control of robust design in multiobjective optimization under uncertainties. *Struct Multidisciplinary Optim,* vol. 45, pp. 247–256.

Graham, L.L.; Siragy, E.F. (2001): Stochastic finite-element analysis for elastic buckling of stiffened panels. *J Eng Mech,* vol. 127, pp. 91-97.

He, J.; Liu, Y.; Chen, A.; Yoda, T. (2012a): Shear behavior of partially encased composite I-girder with corrugated steel web: experimental study. *J Constr Steel Res,* vol. 77, pp. 193-209.

He, J.; Liu, Y.; Lin, Z.; Chen, A.; Yoda, T. (2012b): Shear behavior of partially

encased composite I-girder with corrugated steel web: numerical study. *J Constr Steel Res*, vol. 79, pp. 166-182.

Huang, L.; Hikosaka, H.; Komine, K. (2004): Simulation of accordion effect in corrugated steel web with concrete flanges. *Comput & Struct*, vol. 82, pp. 2061-2069.

Johnson, R.P.; Cafolla, J. (1997): Local flange buckling in plate girders with corrugated webs. *Struct & Build,* ICE vol. 123, pp. 148-156.

Kamiński, M. (2007): Generalized perturbation-based stochastic finite element method in elastostatics. *Comp & Struct*, vol. 85, pp. 586-594.

Kamiński, M. (2011a): Homogenization of fiber-reinforced composites with random properties using the weighted least squares response function approach. *Arch. Mech,* vol. 63, pp. 479–505.

Kamiński, M. (2011b): Structural sensitivity analysis in nonlinear and transient problems using the local response function technique. *Struct Multidisciplinary Opt*, vol. 43, pp. 261-274.

Kamiński, M. (2013): The stochastic perturbation method for computational mechanics. Wiley & Sons, Chichester.

Kamiński, M.; Szafran J. (2010): Random eigenvibrations of elastic structures by the response function method and the generalized stochastic perturbation technique. *Arch Civil & Mech. Engrg,* vol. 10, pp. 33–48.

Kamiński, M.; Świta, P. (2011): Generalized stochastic finite element method in elastic stability problems. Comput & Struct, vol. 89, pp. 1241-1252.

Kiymaz, G.; Coskun, E.; Cosgun, C.; Seckin, E. (2010): Transverse load carrying capacity of sinusoidally corrugated steel web beams with web openings. *Steel & Comp Struct*, vol. 10, pp. 69-85.

Kleiber, M. (1986): Introduction to the finite element method (in Polish), Polish Scientific Publishers, Warszawa - Poznań.

Luo, R.; Edlund, B. (1994): Buckling of trapezoidally corrugated panels using spline finite strip method. *J Thin Walled Struct*, vol. 18, pp. 200-209.

Melchers, R.E.; Horwood, E. (1987): Structural reliability. Analysis and prediction, Wiley & Sons, Chichester.

Mendera, Z.; Kuchta, K. (2002): Profiles with SIN corrugated-web (in Polish), Technical University of Cracow Press, Cracow.

Mironowicz, W.; Śniady, P. (1987): Dynamics of machine foundations with random parameters. *J Sound Vibr*, vol. 112, pp. 23-30.

Moller, B.; Beer, M. (2004): Fuzzy randomness. Uncertainty in civil engineering

and computational mechanics, Springer Verlag, Berlin-Heidelberg.

Murzewski, J. (1989): Reliability of civil engineering structures (in Polish), Arkady, Warszawa.

Papadopoulos, V.; Stefanou, G.; Papadrakakis, M. (2009): Buckling analysis of imperfect shells with stochastic non-Gaussian material and thickness properties. *Int J Sol & Struct*, vol. 46, pp. 2800-2808.

Sadovský, Z.; Drdácký, M. (2001): Buckling of plate strip subjected to localized corrosion—A stochastic model. *J Thin-Walled Struct*, vol. 39, pp. 247-259.

Sayed-Ahmed, E.Y. (2001): Behaviour of steel and/or composite girders with corrugated steel webs. *Can J Civil Engrg*, vol. 28, pp. 656-672.

Shinozuka, M.; Astill, C.J. (1972): Random eigenvalue problems in structural analysis, *AIAA J*, vol. 10, pp. 456-462.

Spanos, P.D.; Ghanem, R. (1991): Stochastic finite elements. A spectral approach, Springer-Verlag, Berlin-Heidelberg.

Steinböck, A.; Jia, X.; Höfinger, G.; Rubin, H.; Mang, H.A. (2008): Remarkable postbuckling paths analyzed by means of the consistently linearized eigenproblem. *Int J Num Meth Engrg*, vol. 76, pp. 156–182.

Waarts, P.H.; Vrouwenvelder, A.C.W.M.; (1999): Stochastic finite element analysis of steel structures. *J Constr Steel Res,* vol. 52, pp. 21–32.